Entropy-scaling based pseudo-component viscosity and thermal conductivity models for hydrocarbon mixtures and fuels containing iso-alkanes and two-ring saturates

Houman B. Rokni[1, 2], Joshua D. Moore[1], and Manolis Gavaises[2]

[1] Afton Chemical Corp., Richmond, Virginia 23219, USA

[2] Department of Mechanical Engineering and Aeronautics, City, University of London, Northampton Square, EC1V 0HB London, UK

Abstract

Recently, Rokni et al. [1, 2] developed entropy-scaling based pseudo-component techniques to predict the viscosity and thermal conductivity of hydrocarbon mixtures and fuels up to high temperature and pressure conditions using only two calculated or measured mixture properties (number average molecular weight and hydrogen-to-carbon ratio). The models are accurate for many hydrocarbon mixtures that do not contain branched compounds (7 and 2% mean absolute percent deviation (MAPD) for viscosity and thermal conductivity, respectively, on average). However, predictions for some hydrocarbon mixtures and fuels containing iso-alkanes are often less accurate (16 and 19% MAPD for viscosity and thermal conductivity, respectively, on average). To improve predictions, it was proposed [1, 2] to fit one model parameter using an experimental reference viscosity or thermal conductivity data point, which may not be ideal if experimental reference data are not available. In order to make these models more practical, this study fits empirical correlations for the model parameters, so that accurate predictions can be made without

[1]Corresponding author, e-mail: joshua.moore@aftonchemical.com

fitting model parameters. The correlations enable viscosity and thermal conductivity predictions for a wide range of hydrocarbon mixtures and fuels, including those containing branched alkanes, and no longer require input of any experimental reference viscosity or thermal conductivity data. The correlations are temperature (fit to data from 288 to 550 K) and pressure (fit to data from 1 to 4,400 bar) dependent and are functions of average molecular weight, hydrogen-to-carbon ratio, iso-alkane and two-ring saturate concentrations. Viscosity and thermal conductivity predictions were found to improve to within 5 and 2% average MAPD, respectively, relative to experimental data for the hydrocarbon mixtures and fuels considered in this study.

Introduction

Thermophysical property models are used within computational fluid dynamics (CFD) to assess the performance, emissions, and fuel economy of engines [3-10]. The accuracy of these CFD models depends on accurate representation of the thermophysical fuel properties, especially viscosity and thermal conductivity, often up to extreme pressure conditions. Various viscosity [1, 11, 12] and thermal conductivity [2, 13, 14] models have been proposed for fuels in the literature. These models range from empirical [15-22] to mixture [23] and pseudo-component models [1, 2, 13, 14, 24-35], such as expanded fluid theory (EFT) [13, 14, 25-28], friction theory (FT) [29-33], and free volume theory (FVT) [34, 35].

Recently, Rokni et al. [1, 2] developed an entropy-scaling based pseudo-component (ESBPC) technique to predict viscosity and thermal conductivity of well-characterized hydrocarbon mixtures and fuels (including rocket propellant, jet, and diesel fuels) up to high temperature and high pressure (HTHP) conditions, using the perturbed-chain statistical associating fluid theory (PC-SAFT) equation of state (EoS) [36]. The models define a single pseudo-component to represent the compounds in a hydrocarbon mixture or fuel and at minimum, require the input of

two experimentally measured or calculated inputs (two-input parameter (2IP) model): the mixture number average molecular weight ($MW_{mixture}$) and hydrogen to carbon ratio (HN/CN). While the 2IP model is accurate for many hydrocarbon mixtures containing components from different chemical families (e.g., normal-alkanes, benzenes, naphthalenes, cyclohexanes), viscosity and thermal conductivity predictions for some mixtures containing iso-alkanes are less accurate, with up to 24% mean absolute percent deviation (MAPD) calculated for diesel, rocket propellant and jet fuels [1, 2]. Predictions are improved for mixtures containing branched alkanes by fitting one model parameter to a data point at a reference condition (e.g., data point at the lowest available temperature and pressure). This three-input parameter (3IP) model predicted viscosity and thermal conductivity with 4 and 2% MAPD on average, respectively, for several hydrocarbon mixtures and fuels [1, 2].

However, experimental viscosity and thermal conductivity reference data are often not available for every mixture or fuel. The ESBPC technique would be more practical to use if the accuracy of predictions were improved for hydrocarbon mixtures and fuels containing branched alkanes but did not require fitting model parameters or input of experimental viscosity or thermal conductivity reference data. This study achieves this by replacing the ESPBC model's thermal conductivity and viscosity coefficients with empirical correlations, such that accurate viscosity and thermal conductivity predictions up to HTHP conditions no longer require fitting of model parameters or input of experimental viscosity or thermal conductivity reference data, even for hydrocarbon mixtures and fuels containing branched alkanes. These empirical correlations explicitly account for concentrations of iso-alkanes and two-ring saturates, such as decalin derivative compounds. This Entropy Scaling Coefficient Corrected (ESCC) model requires three mixture property inputs ($MW_{mixture}$, HN/CN, and weight fraction of iso-alkanes in the mixture ($wt_{iso-alkanes}$)) for thermal conductivity predictions and four mixture property inputs

($MW_{mixture}$, HN/CN, $wt_{iso-alkanes}$, and weight fraction of two-ring saturates in the mixture ($wt_{two-ring\ saturates}$)) for viscosity predictions. The iso-alkane and two-ring saturate chemical families are selected based upon understanding that the ESPBC technique does not distinguish the difference between normal and branched alkanes [1, 2]. Including the two-ring saturates in the correlation is observed to improve the viscosity predictions. When using the ESCC model, viscosity predictions (298 to 533 K and up to 2,600 bar) are within 5% MAPD, on average, which is comparable to the uncertainty of the experimental data for the hydrocarbon mixtures (2%) and diesel fuels (up to 4%) in this study. The thermal conductivity predictions (288 to 550 K and up to 4,400 bar) are 2% MAPD, on average, for the ESCC model, which is comparable to the uncertainty of the experimental data for the hydrocarbon mixtures (1%) and rocket propellant and jet fuels (3%) in this study.

Hydrocarbon Mixtures

Table 1 lists the studies which measured the viscosity of hydrocarbon mixtures up to high pressures and temperatures. Dauge et al. [37] reported viscosity measurements for seven compositions of binary mixtures (referred to as M1) containing 2,2,4,4,6,8,8-heptamethylnonane (i.e., isocetane, referred to as HMN) and n-tridecane (nC13) from 293 to 353 K and up to 1,000 bar. Zéberg-Mikkelsen et al. [38] measured viscosity of thirteen compositions of ternary mixtures (referred to as M2) containing methyl-cyclohexane (MCH), decalin, and HMN from 293 to 353 K and up to 1,000 bar. Ducoulombier et al. [39] reported viscosity for a quaternary mixture (referred to as M3) containing n-decane (nC10), n-dodecane (nC12), n-tetradecane (nC14), and n-hexadecane (nC16) from 313 to 353 K and up to 1,000 bar. Zéberg-Mikkelsen et al. [40] reported viscosity measurements for 21 compositions of ternary mixtures (referred to as M4) containing

HMN, nC13, and methylnaphthalene (MNP) up to 353 K and 1,000 bar. Boned et al. [41] reported viscosity measurements for a ternary (referred to as M5) and a quinary (referred to as M6) mixture from 293 to 353 K and up to 1,000 bar.

Table 1. Weight fractions of compounds in the mixtures considered in this study for viscosity [37-41].

Compound	Chemical Family	M1	M2	M3	M4	M5	M6
n-heptane	n-alkanes	-	-	-	-	-	-
n-decane	n-alkanes	-	-	0.193	-	-	-
n-dodecane	n-alkanes	-	-	0.231	-	-	-
n-tridecane	n-alkanes	0.104-0.851	-	-	0.109-0.750	0.400	0.200
n-tetradecane	n-alkanes	-	-	0.269	-	-	-
n-hexadecane	n-alkanes	-	-	0.307	-	-	-
2,2,4,4,6,8,8-heptamethylnonane	iso-alkanes	balance	balance	-	0.154-0.806	-	0.200
methylcyclohexane	cyclohexanes	-	0.062-0.618	-	-	-	-
heptylcyclohexane	cyclohexanes	-	-	-	-	0.349	0.350
decalin	decalins	-	0.087-0.719	-	-	-	-
heptyl benzene	benzenes	-	-	-	-	0.250	0.150
methylnaphthalene	naphthalenes	-	-	-	balance	-	0.100

Table 2 lists the studies which report the thermal conductivity of hydrocarbon mixtures up to high temperatures and pressures. Wakeham et al. [42] reported thermal conductivity for binary mixtures containing benzene and trimethylpentane (TMP) (referred to as M7) for two different compositions at temperatures from 313 to 345 K and pressures up to 3,500 bar. Fareleira et al. [43] and Wakeham et al. [42] reported thermal conductivity data for binary mixtures containing n-heptane (C7) and TMP (referred to as M8) for three different compositions at temperatures from 308 to 360 K and pressures up to 4,500 bar. Wada et al. [44] reported thermal conductivity data for binary mixtures containing C7 and n-undecane (C11), C7 and C16, and C11 and C16 (referred to as M9, M10, and M11, respectively) for three different compositions for each mixture at atmospheric pressure and temperatures from 295 to 345 K. Wada et al. [44] also reported thermal

conductivity for ternary mixtures (referred to as M12) including C7, C11, and C16 for three compositions at a range of temperatures from 295 to 345 K and 1 bar.

Table 2. Weight fractions of compounds in the mixtures considered in this study for thermal conductivity [42-44].

Compound	Chemical Family	M7	M8	M9	M10	M11	M12
n-heptane	n-alkanes	-	0.456-0.726	0.658-0.342	-	0.430-0.871	0.052-0.462
n-undecane	n-alkanes	-	-	balance	0.187-0.674	-	0.242-0.361
n-hexadecane	n-alkanes	-	-	-	balance	balance	balance
trimethylpentane	iso-alkanes	0.328-0.814	balance	-	-	-	-
benzene	benzenes	balance	-	-	-	-	-

Fuels

Aquing et al. [11] reported viscosity of two diesel fuels (referred to as Middle East Straight Run (MESR) and Highly Naphthenic (HNA)) from 323 to 423 K and up to 3,500 bar. Rowane et al. [45] measured viscosity of three diesel fuels (referred to as Highly Paraffinic (HPF), Ultra-Low Sulfur Diesel (ULSD), and Highly Aromatic (HAR)) up to 533 K and 3,000 bar. Akhmedova-Azizova et al. [46] reported the thermal conductivity of RP1 fuel at temperatures between 293 and 598 K and pressures up to 600 bar. Bruno [47] measured the thermal conductivity of RP2 fuel over a wide range of temperatures from 300 to 550 K and pressures up to 600 bar. Xu et al. [48] reported thermal conductivity measurements of RP3 fuel at temperatures from 285 to 513 K and pressures up to 50 bar. Jia et al. [49] reported the thermal conductivity of RP3 fuel at temperatures from 311 to 399 K and a single isobar at 30 bar. Bruno [50] also measured the thermal conductivity of three different jet fuels, including JP-8 3773 (referred to as JP-8) and Jet A 4658 (referred to as Jet A) at high temperatures from 270 to 470 K and pressures up to 400 bar. The detailed chemical family compositions of the rocket propellant and jet fuels are reported elsewhere (RP1 [51], RP2 [51], RP3 [51], Jet A [52], and JP-8 [52]).

ESBPC Technique for Viscosity and Thermal Conductivity Predictions:

The two-input parameter (2IP) techniques for viscosity and thermal conductivity predictions are briefly described here but are explained in greater detail in ref. [1, 2]. Residual entropy, $\tilde{s}^{\mathrm{res}}$, (the difference between the real fluid and ideal gas entropy) (Eq. (1)) (i.e., molar residual entropy, $\bar{s}^{\mathrm{res}}$, divided by the gas constant, *R*), in temperature (*T*) and volume (*V*) state variables, is calculated from the residual Helmholtz free energy, $\tilde{a}^{\mathrm{res}}$ (the difference between the real fluid and ideal gas Helmholtz free energy), using the PC-SAFT EoS.

$$\tilde{s}^{\mathrm{res}}(V,T) = -\left(\frac{\partial \tilde{a}^{\mathrm{res}}}{\partial T}\right)_V \tag{1}$$

The pseudo-component PC-SAFT parameters, m, σ, and ε/k, needed to calculate $\tilde{s}^{\mathrm{res}}$ are determined using the pseudo-component technique and correlations shown in the supporting information (SI). Using entropy-scaling, first proposed by Rosenfeld [53], a third-order polynomial, proposed by Lötgering-Lin and Gross [54] (Eq. 2), is used to correlate the reduced transport property (i.e., α^*, viscosity (η) or thermal conductivity (λ)) to reduced residual entropy (s^*) (Eq. 3).

$$\ln(\alpha^*) = \ln\left(\alpha/\alpha_{CE}\right) = A + Bs^* + C{s^*}^2 + D{s^*}^3 \tag{2}$$

$$s^* = \left(\frac{\tilde{s}^{res}(V,T)}{m}\right) \tag{3}$$

In Eq. (2), α_{CE} is the Chapman-Enskog viscosity or thermal conductivity [55-57]. The coefficients (i.e., A, B, C, and D) in Eq. (2) are first calculated for an n-alkane and a poly-nuclear aromatic (PNA) with the same number average molecular weight as the mixture ($\mathrm{MW_{mixture}}$) using correlations shown in the SI. Next, the pseudo-component coefficients are calculated by averaging

contributions of the n-alkane and PNA (using Eqs. (4 and 5) for viscosity and thermal conductivity models, respectively), which uses an averaging parameter, Z, defined as a function of the mixture degree of unsaturation ($\mathrm{DoU}_{\mathrm{mixture}}$). The procedure to calculate Z is provided in the SI.

$$\left(F \times m^2\right)_{\mathrm{pseudo-component}} = (1-Z) \times \left(F \times m^2\right)_{\mathrm{n-alkane}} + Z \times \left(F \times m^2\right)_{\mathrm{PNA}} \quad (4)$$

$$(F)_{\mathrm{pseudo-component}} = (1-Z) \times (F)_{\mathrm{n-alkane}} + Z \times (F)_{\mathrm{PNA}} \quad (5)$$

where F is the coefficient A, B, C, or D in Eq. (2). For mixtures containing iso-alkanes, the three-input parameter (3IP-1) model, proposed in ref. [1, 2], fits one model parameter (D for viscosity or B for thermal conductivity) to reproduce a single data point at a chosen reference state, instead of calculating it using Eqs. (4 and 5). All model parameters needed to predict viscosity and thermal conductivity for all hydrocarbon mixture compositions and fuels, in this study, are reported in the SI.

Entropy Scaling Coefficient Corrected (ESCC) Model

In this study, a new model is proposed (referred to as the Entropy Scaling Coefficient Corrected (ESCC) model), which correlates the pseudo-component coefficients, instead of calculating them using Eqs. (4 and 5). The pseudo-component coefficients are correlated to mixture properties ($\mathrm{MW}_{\mathrm{mixture}}$ and HN/CN) and weight fractions of iso-alkanes (i.e., heptamethylnonane and trimethylpentane in this study) and two-ring saturates (i.e., decalin in this study). Training set data was used to fit the G_i coefficients in Eq. (6) for viscosity and Eq. (7) for thermal conductivity. The training set for the ESCC viscosity coefficient correlations (Eq. 6) contained a subset of mixtures M1, M2, M4 as well as mixtures M3, M5, and M6 (690 total data points). The training set for the ESCC thermal conductivity coefficient correlations (Eq. 7) contained a subset of mixtures

M7, M8, M9, M10, and M12 (134 total data points). The correlations were then validated for the remaining mixtures and fuels as a test set (356 thermal conductivity data points and 1134 viscosity data points). Tables 3 and 4 list the parameters in Eqs. (6 and 7) for the viscosity and thermal conductivity ESCC models, respectively.

$$G_\eta = G_{\eta_1} \times MW_{mixture} + G_{\eta_2} \times {}^{HN}/_{CN} + G_{\eta_3} \times \mathrm{wt}_{\mathrm{iso-alkanes}} + G_{\eta_4} \times \mathrm{wt}_{\mathrm{two-ring\,saturates}} + G_{\eta_5} \quad (6)$$

$$G_\lambda = G_{\lambda_1} \times MW_{mixture} + G_{\lambda_2} \times {}^{HN}/_{CN} + G_{\lambda_3} \times \mathrm{wt}_{\mathrm{iso-alkanes}} + G_{\lambda_4} \quad (7)$$

In Eqs. (6 and 7) G_η and G_λ are the pseudo-component coefficients (A, B, C, or D) in Eq. (2), which are a function of $\mathrm{MW_{mixture}}$, HN/CN, and weight fraction (wt) of iso-alkanes ($\mathrm{wt_{iso-alkanes}}$) and two-ring saturates ($\mathrm{wt_{two-ring\,saturates}}$). Inclusion of the two-ring saturate concentration was observed to improve the viscosity predictions using the ESCC correlation. For thermal conductivity predictions, a lack of available hydrocarbon mixture data containing two-ring saturates in the literature precluded including $\mathrm{wt_{two-ring\,saturates}}$ in Eq. (7). The multilinear regression in Eqs. (6 and 7) yielded satisfactory predictions for all mixture compositions based upon MAPD.

Table 3. Parameters needed to calculate the coefficients (G_{η_i}) in Eq. (6) as a function of $\mathrm{MW_{mixture}}$, HN/CN, $\mathrm{wt_{iso-alkanes}}$, and $\mathrm{wt_{two-ring\,saturates}}$ for the viscosity ESCC model: An average MAPD of 4.0% is obtained for viscosities using Eq. (6) for the mixture compositions used in the training set (690 data points).

G_{η_i}	G_{η_1}	G_{η_2}	G_{η_3}	G_{η_4}	G_{η_5}
A	3.267×10^{-1}	-1.711×10^{0}	4.210×10^{-2}	1.359×10^{-1}	8.249×10^{-2}
B	3.236×10^{-1}	-1.605×10^{0}	1.835×10^{-2}	-5.758×10^{-2}	-3.786×10^{0}
C	3.261×10^{-1}	-2.596×10^{-1}	3.770×10^{-2}	8.726×10^{-2}	-2.273×10^{0}
D	-5.428×10^{-3}	1.432×10^{-2}	-8.926×10^{-3}	-1.973×10^{-2}	-4.498×10^{-1}

Table 4. Parameters needed to calculate the coefficients (G_{λ_i}) in Eq. (7) as a function of $MW_{mixture}$, HN/CN, and $wt_{iso-alkanes}$ for the thermal conductivity ESCC model: An average MAPD of 2.2% is obtained for thermal conductivities using Eq. (7) for the mixture compositions used in the training set (134 data points).

G_{λ_i}	G_{λ_1}	G_{λ_2}	G_{λ_3}	G_{λ_4}
A	-4.798×10^{-1}	3.524×10^{-1}	-1.298×10^{-1}	7.313×10^{-1}
B	-2.261×10^{-2}	-2.183×10^{-2}	7.079×10^{-2}	-1.440×10^{-1}
C	5.153×10^{-1}	-2.431×10^{-1}	-2.523×10^{-2}	3.628×10^{-1}
D	1.894×10^{-1}	-7.804×10^{-2}	-1.064×10^{-2}	5.156×10^{-2}

Results and Discussion

Viscosities and thermal conductivities were predicted for the hydrocarbon mixtures and fuels in this study using the 2IP model, the ESCC model using Eqs. (6 and 7), the 3IP model, and two additional variations of the 2IP model. One variation of the 2IP model (referred to as 2IP-1Pfit) fits a single model parameter (coefficient B in the thermal conductivity model or D in the viscosity model) to minimize the average MAPD of the whole data set for each mixture. The second variation (referred to as 2IP-4Pfit) fits all four model parameters (A, B, C, and D) in Eq. (2) to minimize the average MAPD of the whole data set for each mixture and represents the best possible fit of Eq. (2) to the experimental data. The predictions using the 2IP, 2IP-1Pfit, and ESCC models are shown in the subsequent figures for selected mixtures. However, predictions for all available mixture data for the ESCC, 2IP, 3IP, 2IP-1Pfit, and 2IP-4Pfit models are provided in the supplementary information (SI).

Figure 1 shows viscosity predictions using the 2IP, 2IP-1Pfit, and ESCC models in this study compared to experimental data for representative hydrocarbon mixtures and fuels, which contain a wide range of iso-alkane and two-ring saturate concentrations. M1-4 contains 55.1 wt% iso-alkanes, and the 2IP model predicts viscosity with 10.0% MAPD, whereas the 3IP, 2IP-1Pfit,

and ESCC models predict viscosity with MAPDs of 2.7, 2.6, and 2.3%, respectively. M2-9 contains 32.7 wt% iso-alkanes and 20.0 wt% two-ring saturates, and viscosity is predicted with 25.7% MAPD using the 2IP model and 4.5% MAPD using the ESCC model. Viscosity predictions improve over the ESCC model to 3.1 and 2.1% MAPD using the 3IP and 2IP-1Pfit models, respectively but require experimental reference data to fit model parameters. M4-1 contains 80.6 wt% iso-alkanes, and the 2IP model predicts viscosity with 17.8% MAPD, whereas the 3IP, 2IP-1Pfit, and ESCC models provide MAPDs of 8.1, 5.5, and 3.9%, respectively. The MESR diesel fuel contains 27.3 wt% iso-alkanes and 4.8 wt% two-ring saturates, and the 2IP model predicts viscosity with 13.4% MAPD. The 3IP and 2IP-1Pfit models slightly improve predictions to 11.6 and 11.1% MAPD, respectively, while the ESCC model improves predictions further to 9.2% MAPD. Similar observations are found for the other diesel fuels and mixtures. Table 5 compares the MAPDs for viscosity predictions averaged over all mixtures and compositions using the ESCC model (4.8%), 2IP (15.0%), 3IP (5.5%), 2IP-1Pfit (4.1%), and 2IP-4Pfit (1.9%) models. The required input parameters, as well as the MAPDs for viscosity predictions for all models, are reported in the SI for all hydrocarbon mixture compositions and diesel fuels in this study.

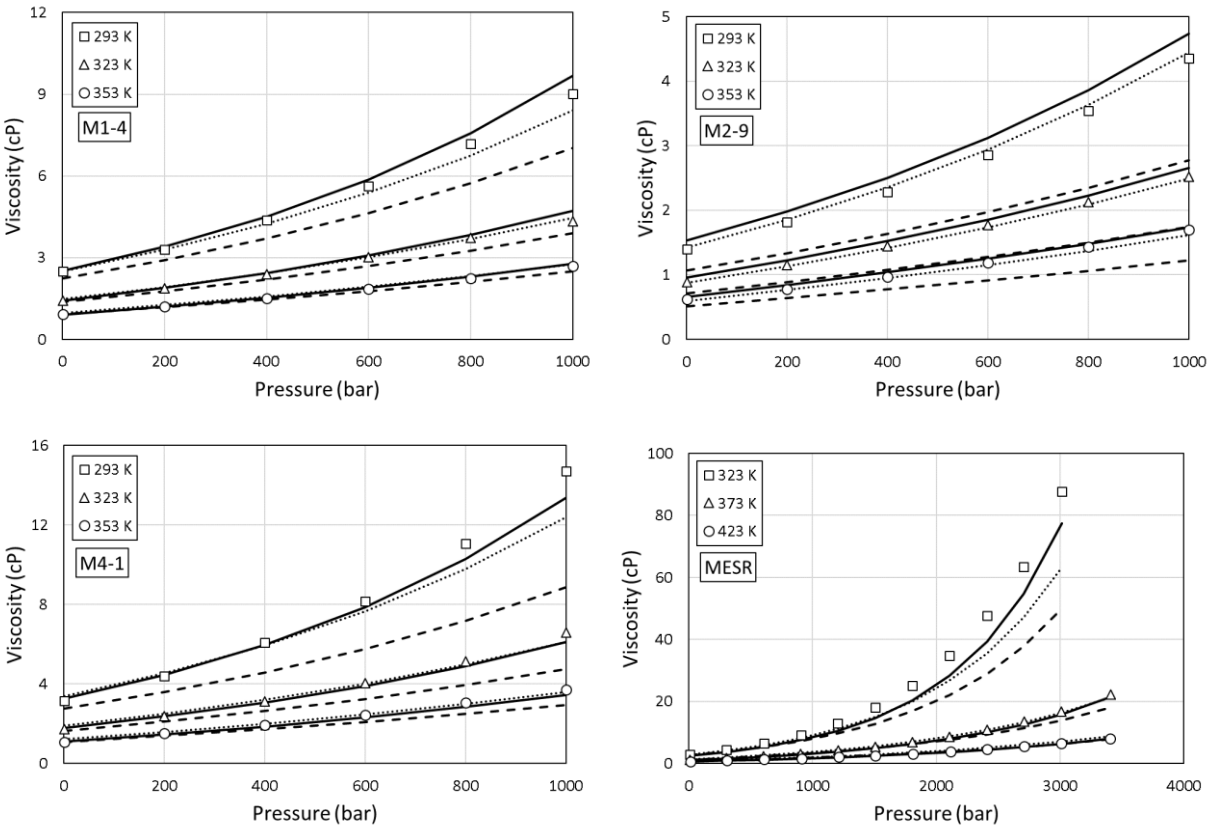

Figure 1. Pseudo-component viscosity predictions compared to experimental data [11, 37, 38, 40] (symbols) for selected hydrocarbon mixtures (M1-4, M2-9, and M4-1) and diesel fuel MESR using the 2IP (dashed lines), 2IP-1Pfit (dotted lines), and ESCC (solid lines) models. Results for the 3IP and 2IP-4IPfit models are listed in the SI but are not shown here to prevent cluttered graphs. Note that the y-axis and x-axis scales are different in each figure.

Table 5. The MAPD (%) for pseudo-component viscosity predictions using the 2IP, 3IP, 2IP-1Pfit, 2IP-4Pfit, and ESCC pseudo-component models.

Mixture or Fuel	2IP	2IP-4Pfit	3IP	2IP-1Pfit	ESCC
M1	13.9	1.8	3.6	5.6	3.6
M2	33.8	2.6	3.6	5.4	4.3
M3	5.3	2.3	2.9	3.0	6.1
M4	5.7	1.3	3.3	4.4	4.6
M5	7.1	1.9	2.3	3.4	7.0
M6	4.3	1.6	1.6	2.1	8.5
MESR	13.4	4.5	11.1	11.6	9.2
HNA	13.3	0.9	10.9	11.5	9.7
HPF	14.1	3.3	13.8	15.1	5.2
ULSD	12.2	3.8	8.3	9.5	7.0
HAR	12.9	2.6	12.2	12.3	5.4
Average	15.0	1.9	4.1	5.5	4.8

Figure 2 shows thermal conductivity predictions using the 2IP, 2IP-1Pfit, and ESCC models compared to the experimental data for representative hydrocarbon mixtures and fuels ranging from 0 to 100 wt% iso-alkanes. M7-1 contains 81.4 wt% iso-alkanes, and the 2IP model predicts thermal conductivity with 33.3% MAPD, whereas the 3IP, 2IP-1Pfit, and ESCC models provide MAPDs of 2.5, 1.1, and 3.9%, respectively. M8-2 contains 28.2 wt% iso-alkanes, and thermal conductivity is predicted with 18.4% MAPD using the 2IP model. Thermal conductivity predictions improve to 4.7 and 3.1% MAPD using the 3IP and 2IP-1Pfit models, but the ESCC model improves the MAPD further to 2.3%. M11-1 contains only normal alkanes, and the 2IP model predicts thermal conductivity with 4.4% MAPD. The 3IP and 2IP-1Pfit models provide slightly improved thermal conductivity predictions for M11-1 (1.6 and 1.4% MAPDs for 3IP and 2IP-1Pfit models, respectively) compared to 2.3 % MAPD for the ESCC model. However, the 3IP and 2IP-1Pfit models require the input of experimental thermal conductivity reference data. The RP1 fuel contains 36.6 wt% iso-alkanes, and the 2IP model predicts thermal conductivity with 20.4% MAPD. The 3IP and 2IP-1Pfit models improve predictions to 1.7 and 1.5% MAPD, while

the ESCC model predicts thermal conductivity with a 3.9% MAPD. Similar observations are found for other hydrocarbon mixtures and fuels. Table 6 lists the MAPDs for thermal conductivity predictions using the models for each hydrocarbon mixture (averaged over all compositions) and fuel. The MAPDs for thermal conductivity predictions averaged over all mixtures and compositions using the ESCC model (2.2%) are compared with the 2IP (9.3%), 3IP (2.4%), 2IP-1Pfit (1.6%), and 2IP-4Pfit (0.5%) models. The required input parameters, as well as the MAPDs for thermal conductivity predictions for all models, are reported in the SI for all hydrocarbon mixture compositions and fuels in this study.

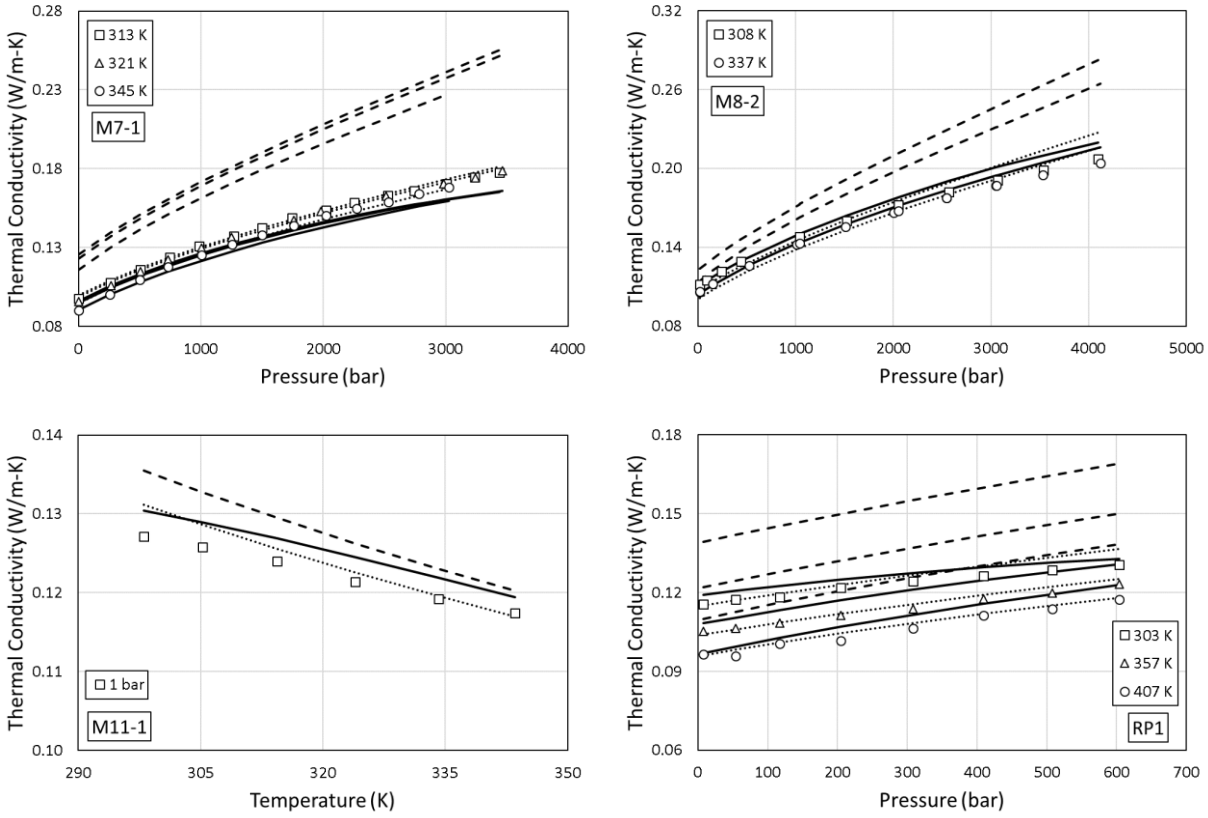

Figure 2. Pseudo-component thermal conductivity predictions compared to experimental data [42-44, 46] (symbols) for selected hydrocarbon mixtures (M7-1, M8-2, and M11-1) and fuel RP1 using the 2IP (dashed lines), 2IP-1Pfit (dotted lines), and ESCC (solid lines) models. Results for the 3IP and 2IP-4IPfit models are listed in the SI but are not shown here to prevent cluttered graphs. Note that the y-axis and x-axis scales are different in each figure.

Table 6. The MAPD (%) for pseudo-component thermal conductivity predictions using the 2IP, 3IP, 2IP-1Pfit, 2IP-4Pfit, and ESCC pseudo-component models.

Mixture or Fuel	2IP	2IP-4Pfit	3IP	2IP-1Pfit	ESCC
M7	24.5	0.9	0.9	1.7	2.2
M8	20.9	0.5	2.6	3.8	2.0
M9	1.6	0.3	1.2	1.9	0.8
M10	1.9	0.2	1.9	2.9	1.9
M11	3.2	0.4	1.3	2.2	1.2
M12	2.4	0.2	1.3	2.1	0.6
RP1	20.4	1.0	1.5	1.7	3.9
RP2	23.9	0.6	1.4	1.4	6.0
RP3	9.4	0.6	1.1	1.1	4.8
Jet A	14.6	0.6	2.1	3.4	4.4
JP-8 3773	21.3	0.8	1.0	2.4	5.8
Average	9.3	0.5	1.6	2.4	2.2

Conclusion

The two-input parameter (2IP) entropy-scaling based pseudo-component (ESBPC) model predicts viscosity and thermal conductivity accurately for many hydrocarbon mixtures and fuels (7 and 2% mean absolute percent deviation (MAPD) for viscosity and thermal conductivity, respectively, on average), but often less accurately when mixtures contain branched alkanes, with up to 24% mean absolute percent deviation (MAPD) calculated for fuels. A three-input parameter (3IP) version of the model improves predictions but requires fitting one model parameter using an experimental reference viscosity or thermal conductivity data point, which is not ideal if experimental reference data are not available. To enable more practical yet still accurate predictions, empirical correlations for the entropy-scaling based pseudo-component (ESBPC) coefficients were applied to the ESBPC technique to predict viscosity and thermal conductivity for hydrocarbon mixtures and fuels. Entropy is calculated in this Entropy Scaling Coefficient Corrected (ESCC) model using the pseudo-component technique. However, the viscosity and thermal conductivity coefficients are calculated using empirical correlations fit to a training set of

available high temperature and pressure literature data. The correlations for the thermal conductivity pseudo-component coefficients require three mixture property inputs: the number average molecular weight, hydrogen to carbon ratio, and the weight fraction of iso-alkanes. The correlations for the viscosity pseudo-component correlations require four mixture property inputs: the number averaged molecular weight, hydrogen to carbon ratio, the weight fraction of iso-alkanes, and the weight fraction of two-ring saturates. Training sets of 690 and 134 points were used to fit the correlation parameters for the viscosity and thermal conductivity models, respectively, and a test set of 356 thermal conductivity and 1134 viscosity data points was used to validate the correlations. The ESCC model does not require fitting model parameters to viscosity or thermal conductivity reference data to predict viscosity and thermal conductivity up to high pressures and temperatures, yet viscosities and thermal conductivities are predicted with 4.8 and 2.2% MAPD on average, respectively, which is comparable to the uncertainty of the experimental data for the hydrocarbon mixtures (2%) and fuels (up to 4%) in this study.

Acknowledgments

This project has received funding from the European Union Horizon 2020 Research and Innovation program, Grant Agreement No 675528. The authors wish to thank Ashutosh Gupta (Afton), William B. Anderson (Afton), and Mark McHugh (Virginia Commonwealth University) for their helpful and technical discussions.

References

[1] H.B. Rokni, Moore, J.D., Gupta, A., McHugh, M.A., Gavaises, M., Entropy scaling based viscosity predictions for hydrocarbon mixtures and diesel fuels up to extreme conditions, Fuel, 241 (**2019**) 1203-1213.

[2] H.B. Rokni, Moore, J.D., Gupta, A., McHugh, M.A., Mallepally, R.R., Gavaises, M., General method for prediction of thermal conductivity for well-characterized hydrocarbon mixtures and fuels up to extreme conditions using entropy scaling, Fuel, 245 (**2019**) 594-604.

[3] A. Theodorakakos, Strotos, G., Mitroglou, N., Atkin, C., Gavaises, M., Friction-induced heating in nozzle hole micro-channels under extreme fuel pressurisation, Fuel, 123 (**2014**) 143-150.

[4] C. Rodriguez, Vidal, A., Koukouvinis, P., Gavaises, M., M^{c}Hugh, M.A., Simulation of transcritical fluid jets using the PC-SAFT EoS, Journal of Computational Physics, 374(1) (**2018**) 444-468.
[5] A. Parsa, Srinivasan, S., Saghir, M.Z., Impact of density gradients on the fluid flow inside a vibrating cavity subjected to soret effect, The Canadian Journal of Chemical Engineering, 91(3) (**2013**) 550-559.
[6] C. Rodriguez, Vidal, A., Koukouvinis, P., Gavaises, M., Supercritical and transcritical real-fluid mixing using the PC-SAFT EOS, in: Ilass Europe, 28th Conference on Liquid Atomization and Spray Systems, Valencia, Spain, **2017**, pp. 597-564.
[7] H. An, Yang, W., Li, J., Maghbouli, A., Chua, K.J., Chou, S.K., A numerical modeling on the emission characteristics of a diesel engine fueled by diesel and biodiesel blend fuels, Applied Energy, 130 (**2014**) 458-465.
[8] B. Mohan, Yang, W., Yu, W., Effect of internal nozzle flow and thermo-physical properties on spray characteristics of methyl esters, Applied Energy, 129 (**2014**) 123-134.
[9] A. Maghbouli, Yang, W., An, H., Li, J., Shafee, S., Effects of injection strategies and fuel injector configuration on combustion and emission characteristics of a DI diesel engine fueled by bio-diesel, Renewable Energy, 76 (**2015**) 687-698.
[10] P. Kontoulis, Kaiktsis, L., von Rotz, B., Boulouchos, K., CFD Modeling and Experimental Spray Studies for Different Heavy Fuel Oil Qualities with Respect to Large Two-Stroke Marine Engines, Journal of Energy Engineering, 145(5) (**2019**) 04019014.
[11] M. Aquing, Ciotta, F., Creton, B., Féjean, C., Pina, A., Dartiguelongue, C., Trusler, J.M., Vignais, R., Lugo, R., Ungerer, P., Composition analysis and viscosity prediction of complex fuel mixtures using a molecular-based approach, Energy & Fuels, 26(4) (**2012**) 2220-2230.
[12] C. Schaschke, Fletcher, I., Glen, N., Density and viscosity measurement of diesel fuels at combined high pressure and elevated temperature, Processes, 1(2) (**2013**) 30-48.
[13] F. Ramos-Pallares, Schoeggl, F.F., Taylor, S.D., Yarranton, H.W., Expanded fluid-based thermal conductivity model for hydrocarbons and crude oils, Fuel, 224 (**2018**) 68-84.
[14] F. Ramos-Pallares, Schoeggl, F.F., Taylor, S.D., Yarranton, H.W., Prediction of thermal conductivity for characterized oils and their fractions using an expanded fluid based model, Fuel, 234 (**2018**) 66-80.
[15] O.S. Alade, Ademodi, B., Sasaki, K., Sugai, Y., Kumasaka, J., Ogunlaja, A.S., Development of models to predict the viscosity of a compressed Nigerian bitumen and rheological property of its emulsions, Journal of Petroleum Science and Engineering, 145 (**2016**) 711-722.
[16] S. Eghbali, Dehghanpour, H., Dragani, J., Zhang, X., Phase Behaviour and Viscosity of Bitumen-CO 2/Light Hydrocarbon Mixtures at Elevated Temperatures: A Cold Lake Case Study, in: SPE Canada Heavy Oil Technical Conference, Society of Petroleum Engineers, Calgary, Alberta, Canada, **2018**.
[17] M. Gülüm, Bilgin, A., Measurements and empirical correlations in predicting biodiesel-diesel blends' viscosity and density, Fuel, 199(567-77) (**2017**).
[18] S. Bair, The pressure and temperature dependence of volume and viscosity of four Diesel fuels, Fuel, 135 (**2014**) 112-119.
[19] S.O. Ilyin, Strelets, L.A., Basic Fundamentals of Petroleum Rheology and Their Application for the Investigation of Crude Oils of Different Natures, Energy & Fuels, 32(1) (**2018**) 268-278.
[20] I.P. Kanaveli, Atzemi, M., Lois, E., Predicting the viscosity of diesel/biodiesel blends, Fuel, 199 (**2017**) 248-263.
[21] M. Lapuerta, Rodríguez-Fernández, J., Fernández-Rodríguez, D., Patiño-Camino, R., Modeling viscosity of butanol and ethanol blends with diesel and biodiesel fuels, Fuel, 199 (**2017**) 332-338.

[22] N. Kolev, Multiphase Flow Dynamics 3: Turbulence, Gas Absorption and Release, Diesel Fuel Properties. **2002**, in, Springer Verlag Berlin Heidelberg.
[23] H. Baled, Gamwo, I.K., Enick, R.M., M^{c}Hugh, M.A., Viscosity models for pure hydrocarbons at extreme conditions: A review and comparative study, Fuel, 218 (**2018**) 89-111.
[24] H.B. Rokni, Gupta, A., Moore, J.D., M^{c}Hugh, M.A., Bamgbade, B.A., Gavaises, M., Purely predictive method for density, compressibility, and expansivity for hydrocarbon mixtures and diesel and jet fuels up to high temperatures and pressures, Fuel, 236 (**2019**) 1377-1390.
[25] H.W. Yarranton, Satyro, M.A., Expanded fluid-based viscosity correlation for hydrocarbons, Industrial & Engineering Chemistry Research, 48(7) (**2009**) 3640-3648.
[26] H. Motahhari, Satyro, M.A., Taylor, S.D., Yarranton, H.W., Extension of the expanded fluid viscosity model to characterized oils, Energy & Fuels, 27(4) (**2013**) 1881-1898.
[27] H. Motahhari, Schoeggl, F., Satyro, M., Yarranton, H., Viscosity prediction for solvent-diluted live bitumen and heavy oil at temperatures up to 175-deg-C, Journal of Canadian Petroleum Technology, 52(5) (**2013**) 376-390.
[28] M. Ma, Chen, S., Abedi, J., Modeling the density, solubility and viscosity of bitumen/solvent systems using PC-SAFT, Journal of Petroleum Science and Engineering, 139 (**2016**) 1-12.
[29] S.E. Quiñones-Cisneros, Zéberg-Mikkelsen, C.K., Stenby, E.H., The friction theory (f-theory) for viscosity modeling, Fluid Phase Equilibria, 169(2) (**2000**) 249-276.
[30] S.E. Quiñones-Cisneros, Zéberg-Mikkelsen, C.K., Baylaucq, A., Boned, C., Viscosity modeling and prediction of reservoir fluids: From natural gas to heavy oils, International Journal of Thermophysics, 25(5) (**2004**) 1353-1366.
[31] S.E. Quiñones-Cisneros, Dalberg, A., Stenby, E.H., PVT characterization and viscosity modeling and prediction of crude oils, Petroleum Science and Technology, 22((9-10)) (**2004**) 1309-1325.
[32] K.A. Schmidt, Quiñones-Cisneros, S.E., Kvamme, B., Density and viscosity behavior of a North Sea crude oil, natural gas liquid, and their mixtures, Energy & Fuels, 19(4) (**2005**) 1303-1313.
[33] M.I. Abutaqiya, Zhang, J., Vargas, F.M., Viscosity modeling of reservoir fluids using the Friction Theory with PC-SAFT crude oil characterization, Fuel, 235 (**2019**) 113-129.
[34] Y. Khoshnamvand, Assareh, M., Viscosity Prediction for Petroleum Fluids Using Free Volume Theory and PC-SAFT, International Journal of Thermophysics, 39(4) (**2018**) 54.
[35] Y. Sun, Shen, G., Held, C., Lu, X., Ji, X., Modeling Viscosity of Ionic Liquids with Electrolyte Perturbed-Chain Statistical Associating Fluid Theory and Free Volume Theory, Industrial & Engineering Chemistry Research, 57(26) (**2018**) 8784-8801.
[36] J. Gross, Sadowski, G., Perturbed-chain SAFT: An equation of state based on a perturbation theory for chain molecules, Industrial & Engineering Chemistry Research, 40(4) (**2001**) 1244-1260.
[37] P. Dauge, Canet, X., Baylaucq, A., Boned, C., Measurements of the density and viscosity of the tridecane+ 2, 2, 4, 4, 6, 8, 8-heptamethylnonane mixtures in the temperature range 293.15-353.15 K at pressures up to 100 MPa, High Temerpatures High Pressures, 33(2) (**2001**) 213-230.
[38] C.K. Zéberg-Mikkelsen, Barrouhou, M., Baylaucq, A., Boned, C., High-pressure viscosity and density measurements of the ternary system methylcyclohexane+ cis-decalin+ 2, 2, 4, 4, 6, 8, 8-heptamethylnonane, Journal of Chemical & Engineering Data, 48(6) (**2003**) 1387-1392.
[39] D. Ducoulombier, Zhou, H., Boned, C., Peyrelasse, J., Saint-Guirons, H., Xans, P., Pressure (1-1000 bars) and temperature (20-100. degree. C) dependence of the viscosity of liquid hydrocarbons, The Journal of Physical Chemistry, 90(8) (**1986**) 1692-1700.

[40] C.K. Zeberg-Mikkelsen, Canet, X., Baylaucq, A., Quiñones-Cisneros, S.E., Boned, C., Stenby, E.H., High-pressure viscosity and density behavior of ternary mixtures: 1-methylnaphthalene+ n-tridecane+ 2, 2, 4, 4, 6, 8, 8-heptamethylnonane, International Journal of Thermophysics, 22(6) (**2001**) 1691-1726.
[41] C. Boned, Zéberg-Mikkelsen, C.K., Baylaucq, A., Daugé, P., High-pressure dynamic viscosity and density of two synthetic hydrocarbon mixtures representative of some heavy petroleum distillation cuts, Fluid Phase Equilibria, 212(1) (2003) 143-164.
[42] W.A. Wakeham, Yu, H.R., Zalaf, M., The thermal conductivity of the mixtures of liquid hydrocarbons at pressures up to 400 MPa, International Journal of Thermophysics, 11(6) (**1990**) 987-1000.
[43] J.M.N.A. Fareleira, Li, S.F.Y., Wakeham, W.A., The thermal conductivity of liquid mixtures at elevated pressures, International Journal of Thermophysics, 10(5) (**1989**) 1041-1051.
[44] Y. Wada, Nagasaka, Y., Nagashima, A., Measurements and correlation of the thermal conductivity of liquid n-paraffin hydrocarbons and their binary and ternary mixtures, International Journal of Thermophysics, 6(3) (**1985**) 251-265.
[45] A.J. Rowane, Mahesh, B.V., Rokni, H.B., Moore, J.D., Gavaises, M., Wensing, M., Gupta, A., M^{c}Hugh, M.A., Effect of Composition, Temperature, and Pressure on the Viscosities and Densities of Three Diesel Fuels, Journal of Chemical & Engineering Data, 64(12) (**2019**) 5529-5547.
[46] L.A. Akhmedova-Azizova, Abdulagatov, I.M., Bruno, T.J., Effect of RP-1 compositional variability on thermal conductivity at high temperatures and high pressures, Energy & Fuels, 23(9) (**2009**) 4522-4528.
[47] T.J. Bruno, The Properties of RP-1 and RP-2 MIPR F1SBAA8022G001, **2008**.
[48] G.Q. Xu, Jia, Z.X., Wen, J., Deng, H.W., Fu, Y.C., Thermal-conductivity measurements of aviation kerosene RP-3 from (285 to 513) K at sub-and supercritical pressures, International Journal of Thermophysics, 36(4) (**2015**) 620-632.
[49] Z. Jia, Xu, G., Deng, H., Jie, W., Fu, Y., Experimental measurements of thermal conductivity of hydrocarbon fuels by a steady and kinetic method, Journal of Thermal Analysis and Calorimetry, 123(1) (**2016**) 891-898.
[50] T.J. Bruno, Thermodynamic, Transport and Chemical Properties of Reference JP-8, NIST, **2006**.
[51] R. Xu, Wang, K., Banerjee, S.,Shao, J., Parise, T., Zhu, Y., Wang, S., Movaghar, A., Lee, D.J., Zhao, R., Han, X., Gao, Y., Lu, T., Brezinsky, K., Egolfopoulos, F.N., Davidson, D.F., Hanson, R.K., Bowman, C.T., Wang, H., A physics-based approach to modeling real-fuel combustion chemistry – II. Reaction kinetic models of jet and rocket fuels, Combustion and Flame, 193 (**2018**) 520-537.
[52] J.T. Edwards, Reference jet fuels for combustion testing, in: 55th AIAA Aerospace Sciences Meeting, **2017**, pp. 0146.
[53] Y. Rosenfeld, Relation between the transport coefficients and the internal entropy of simple systems, Physical Review A, 15(6) (**1977**).
[54] O. Lötgering-Lin, J. Gross, Group contribution method for viscosities based on entropy scaling using the perturbed-chain polar statistical associating fluid theory, Industrial & Engineering Chemistry Research, 54(32) (**2015**) 7942-7952.
[55] L. Novak, Self-diffusion coefficient and viscosity in fluids, Journal of Chemical Reactor Engineering, 9(1) (**2011**).
[56] L. Novak, Fluid viscosity-residual entropy correlation, International Journal of Chemical Reactor Engineering, 9(1) (**2011**).
[57] M. Hopp, Gross, J., Thermal Conductivity of Real Substances from Excess Entropy Scaling Using PCP-SAFT, Industrial & Engineering Chemistry Research, 56(15) (**2017**) 4527-4538.